TUDelft

Delft University of Technology

Grain boundary character distribution derived from three-dimensional microstructure reconstruction

Pirgazi, H.; Kestens, LAI

Citation (APA)
Pirgazi, H., & Kestens, LAI. (2015). Grain boundary character distribution derived from three-dimensional microstructure reconstruction. *IOP Conference Series: Materials Science and Engineering*, *82*, [012086]. https://doi.org/10.1088/1757-899X/82/1/012086

Important note
To cite this publication, please use the final published version (if applicable).
Please check the document version above.

PAPER • OPEN ACCESS

Grain boundary character distribution derived from three-dimensional microstructure reconstruction

To cite this article: H Pirgazi and L A I Kestens 2015 *IOP Conf. Ser.: Mater. Sci. Eng.* **82** 012086

View the article online for updates and enhancements.

Related content

- Relationship between Device Performance and Grain Boundary Structural Configuration in a Solar Cell Based on Multicrystalline SiGe
  Noritaka Usami, Wugen Pan, Kozo Fujiwara et al.

- Grain Boundary Character Distribution on the Surface of Cu(In,Ga)Se$_2$ Thin Film
  Takashi Minemoto, Yoichi Wakisaka and Hideyuki Takakura

- Grain boundary misorientation distributions in monoclinic zirconia
  V Y Gertsman, A P Zhilyaev and J A Szpunar

Grain boundary character distribution derived from three-dimensional microstructure reconstruction

H Pirgazi[1] and LAI Kestens[1,2]

[1] Ghent University, Department of Materials Science and Engineering, Technologiepark 903, 9052 Gent, Belgium

[2] Delft University of Technology, Department of Materials Science and Engineering, Mekelweg 2, 2628CD Delft, The Netherlands
E-mail: hadi.pirgazi@ugent.be, leo.kestens@ugent.be

Abstract. Manual serial sectioning which includes consecutive steps of sample preparation and Electron Back Scattering Diffraction (EBSD) measurement was employed to extract the two-dimensional (2D) sections of a pure nickel sample and to reconstruct the three-dimensional (3D) microstructure. A general alignment algorithm based on the minimization of misorientation between two adjacent sections has been developed to accurately align the sections. By employing this alignment algorithm, any in-plane (translational) and rotational misalignment as well as the planparallelity can be corrected. Surface triangulation technique was used to reconstruct the grain boundary surfaces. The Grain Boundary Character Distribution (GBCD) was derived from reconstructed grain boundaries. The results show that a smoother grain boundary plane can be obtained after precise translational and rotational alignment and correction of planparallelity.
The relative grain boundary energy was computed as a function of the five grain boundary parameters based on equilibrium at triple lines. The results show that the grain boundary planes carrying a $\Sigma 3$ type misorientation are dominantly parallel to the {111} crystal plane, which indicates the presence of coherent twin boundaries. It was observed that coherent $\Sigma 3$ type boundaries exhibit the minimum relative grain boundary energy, which is approximately 57% smaller than the average of all $\Sigma 3$ boundaries, including also incoherent twin boundaries.

1. Introduction

Although many microstructural features can be characterized with conventional 2D techniques, there remain many important microstructural properties (e.g. detailed grain boundary features) that can only be measured in three-dimensions (3D). it is well-known that a full description of grain boundary planes is done with 5 parameters: 3 parameters of misorientation across the grain boundary and 2 parameters of the normal to the grain boundary plane [1]. The techniques for 3D characterization of the microstructures are based on two different approaches: (i) observation with high energy radiation and [2, 3] and (ii) by serial sectioning [4-6]. Furthermore, some stereological methods have been proposed and employed to estimate the 3D information from 2D images [7].

Serial sectioning has been the most widely used method to acquire 3D data at the macro/microscale of opaque materials. In this technique, a series of closely spaced parallel sections reveal the third dimension of the microstructure. The usual method for serial sectioning involves the cyclic removal of parallel layers of the sample, followed by imaging (e.g. by EBSD) of the planar sections [4, 8]. The removal of the material for serial sectioning can be performed with different methods: e.g. mechanical polishing, chemical polishing, Focused Ion Beam (FIB) tomography and laser or electrical discharge ablation [5]. Independent of the method employed for the preparation of the sections, the serial sectioning technique suffers from the misalignment between the sections which needs to be accurately corrected before further data processing [9].

The goal of this research is to derive complete grain boundary structural properties and to calculate the relative grain boundary energy for materials with relatively large grain size.

2. Experimental techniques

Wide field 3D Electron Back-Scattering Diffraction (EBSD) was performed on a pure nickel sample by a serial sectioning technique with mechanical polishing. The sample preparation

was done by conventional mechanical polishing to remove a layer with a certain thickness (7 µm). After each polishing step, the EBSD measurements was performed in a high resolution FEG-SEM (of type FEI Quanta™450®) on a large area (3200 ×3200 µm2) with an in-plane step size of 6 µm to obtain the local crystallographic orientations. In order to meticulously fix the scan area on subsequent layers for EBSD measurements, micro-Vickers indentations were used to mark a grid on the sample. These indentations were also used to measure the thickness of each removed layer.

After collecting 50 consecutive sections the 3D volume was reconstructed. Reconstruction was carried out using two algorithms: (i) the first one for precise alignment of the sections and (ii) the second one for the surface meshing of the grain boundary planes by triangulation. An x-y alignment algorithm has been proposed by Lee et al. [10], which is based on the minimization of the average disorientation between two adjacent sections for translational alignment. In this research, this technique is improved by including rotational alignment in addition to the translational alignment. The rotation was carried out by θ° about a rotation axis which was defined by α and β as altitude and azimuth with respect to the sample coordinate system. After each rotation, the scan data were mapped into the new location and the orientations were recalculated by a transformation matrix based on θ° rotation about the axis defined by α and β angles. Figure 1 shows the results of the mentioned alignment procedure. It can be seen that any translational and rotational misalignment as well as the planparallelity (in case of 2 non-parallel consecutive sections which usually appears as a stretched image in the EBSD map) has been precisely corrected.

The second algorithm was used for grain boundary plane triangulation. To this purpose, two grain boundaries between two pairs of corresponding triple junctions were divided into equal segments and triangulation was carried out based on an algorithm proposed by Saylor et al [11].

3. Results and discussion

The results of the reconstructed microstructures are presented in Figure 2. It can be seen that by applying the full alignment procedure (translational plus rotational, cf. Figure 2c), instead of only the translational alignment (cf. Figure 2b) a smoother grain boundary plane is obtained. Together with the improvement of the grain boundary smoothness, the non-uniform orientation spread observed in Figure 2a,b does not appear in Figure 2c. It implies that the full alignment method generates more uniform orientations, which is more realistic for a fully recrystallized structure. This observation is directly related to the correction of the planparallelity and rotational misalignment, which was illustrated in Figure 1.
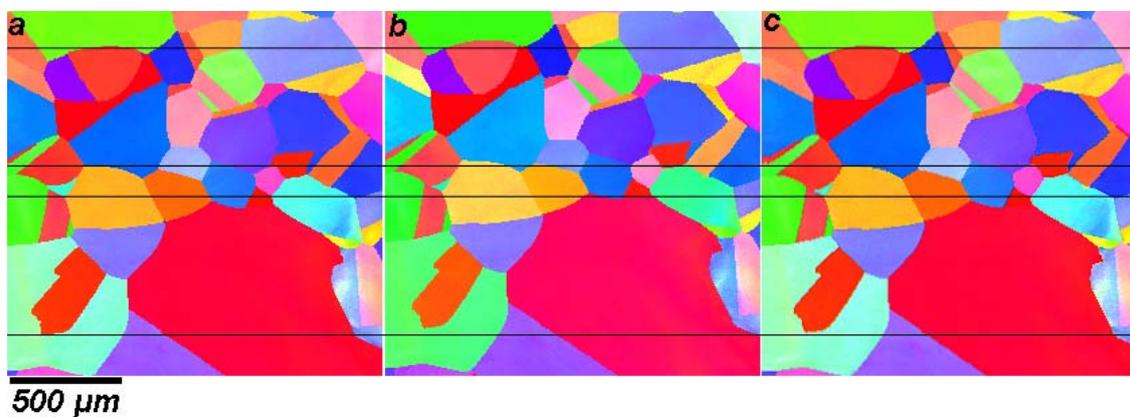

Figure 1. Results of the registration of two consecutive sections, a) the first section is considered as the fixed section, b) the second section after only the translational correction, and c) the second section after translational and rotational alignment. The black lines can be used for comparison between the results.
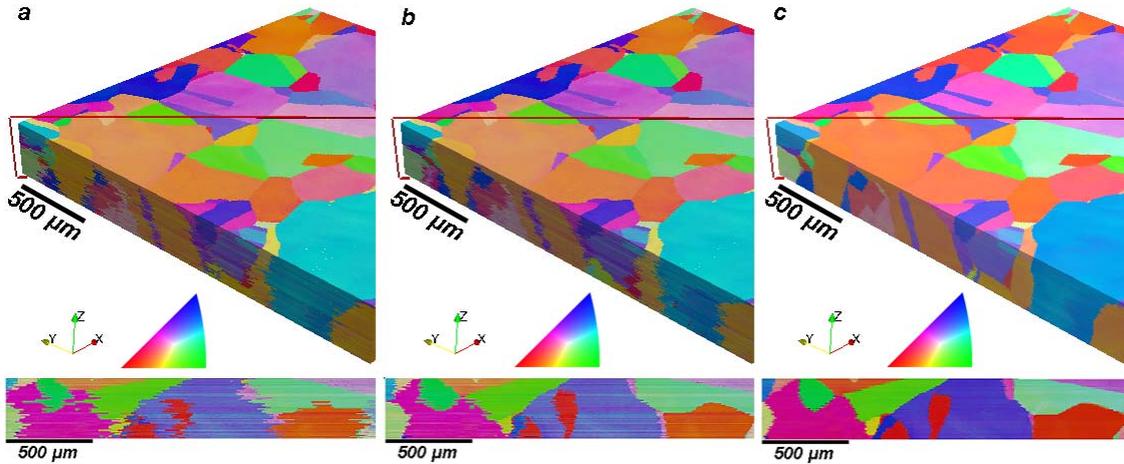
Figure 2. ND inverse pole figure volume of the reconstructed microstructure together with the cross section of the specified plane (red lines), a) the stack of the original EBSD data without any alignment, b) after translational alignment, and c) after translational and rotational alignment.

In order to calculate the grain boundary character distribution, the distribution of the normal to each triangle in the triangulated grain boundary mesh was taken into account. For each type of misorientation, the stereographic projection of the normal to the grain boundary in the crystal reference frame was plotted. Figure 3a and b shows the distribution of the grain boundary planes for Σ3 type of misorientations after translational and full alignment, respectively. It is obvious that a precise alignment of the 2D sections (cf. Figure 3b), which results in a smoother grain boundary plane, gives a more concentrated distribution with higher intensity, whereas the distribution obtained after the translational alignment is very close to the random distribution. The results also show that the grain boundary planes of Σ3 type of misorientations are dominantly terminated by {111} crystal planes, which indicates the presence of coherent twin boundaries. Similar results have been obtained from serial sectioning by FIB tomography [7].

The 3D information was also used to calculate the relative grain boundary energy based on the equilibrium at the triple junctions (Herring's relation). To this purpose, the torque term of the grain boundary energy was calculated using the normal to the grain boundary, whereas the surface tension part was obtained using the tangent to the grain boundary, cf. Equation 1.

$$\sum_{i=1}^{3}\{\sigma_i\hat{t}_i + (\partial\sigma_i/\partial\phi_i)\hat{n}_i\} = \vec{0} \qquad\qquad \text{Eq. 1}$$
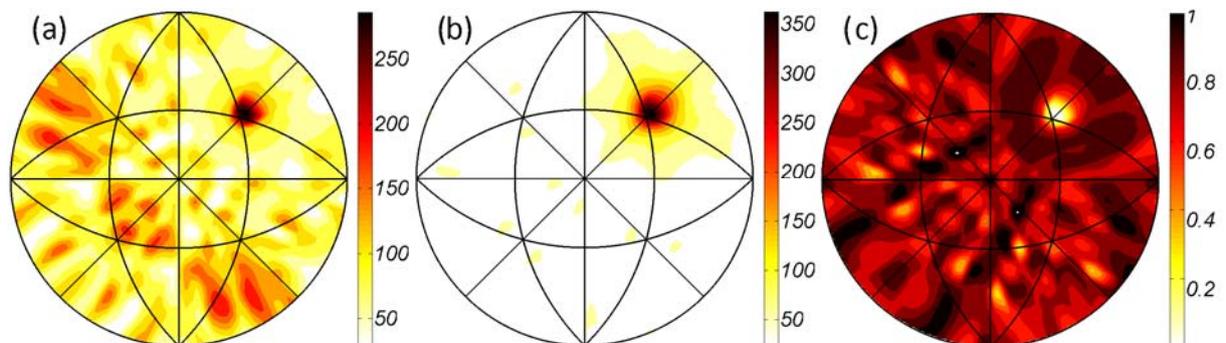

Figure 3. Distribution of grain boundary normals for Σ3 type of misorientation, a) after translational alignment, and b) after translational and rotational alignment. c) Distribution of the relative grain boundary energy for Σ3 type of misorientation.

Where σ_i is the relative grain boundary energy at triple junctions, n_i is the normal to the grain boundary, φ_i is the angle of rotation about triple line and t_i is the tangent to the grain boundary (the cross product of n and triple line).

The relative grain boundary energy was calculated using a method proposed by Adams et al. [12], which is based on discretization of the misorientation space and normal to the grain boundary space and employing multiscale statistical analysis on 3D data sets. The results of this calculation for grain boundaries carrying $\Sigma 3$ type of misorientations is presented in Figure 3c. As expected, the $\Sigma 3$ type of misorientations with coherent twin boundaries (terminated by {111} crystal planes) exhibit the minimum relative grain boundary energy, which is approximately 57% smaller than the average of all $\Sigma 3$ boundaries, including also incoherent twin boundaries.

4. Conclusions

A general alignment algorithm was used to correct in-plane (translational) and rotational misalignment as well as the planparallelity, which resulted in a better reconstruction of the 3D microstructure, illustrated by smoother grain boundary planes. Detailed grain boundary features, including the grain boundary character distribution (GBCD), were calculated from reconstructed grain boundaries. The results show that in a pure nickel sample the grain boundary planes of $\Sigma 3$ type are dominantly terminated by {111} planes, which indicates the presence of coherent twin boundaries. It was also observed that for $\Sigma 3$ type of grain boundaries, the relative grain boundary energy has the minimum value when the grain boundary plane is parallel to {111} plane.

References

[1]　Randle V 2010 Grain boundary engineering: an overview after 25 years Labour Hist. Rev. 26 253-61

[2]　Gault B, Moody M P, Cairney J M and Ringer S P 2012 Atom Probe Microscopy: Springer)

[3]　Miller M K 2005 Handbook of Microscopy for Nanotechnology, ed N Yao and Z L Wang: Kluwer Academic Publisher) pp 227-46

[4]　DeHoff R T 1983 Quantitative serial sectioning analysis: preview Journal of Microscopy 131 259-63

[5]　Zaefferer S, Wright S I and Raabe D 2008 Three-dimensional orientation microscopy in a focused ion beam-scanning electron microscope: A new dimension of microstructure characterization Metall Mater Trans A 39A 374-89

[6]　Uchic M, Groeber M, Shah M, Callahan P, Shiveley A, Scott M, Chapman M and Spowart J 2012 An Automated Multi-Modal Serial Sectioning System for Characterization of Grain-Scale Microstructures in Engineering Materials

[7]　Rohrer G S, Li J, Lee S, Rollett A D, Groeber M and Uchic M D 2010 Deriving grain boundary character distributions and relative grain boundary energies from three-dimensional EBSD data Labour Hist. Rev. 26 661-9

[8]　Alkemper J and Voorhees P W 2001 Quantitative serial sectioning analysis J Microsc-Oxford 201 388-94

[9]　Uchic M D 2011 Computational Methods for Microstructure-Property Relationships, ed S Ghosh and D Dimiduk: Springer US) pp 31-52

[10]　Lee S B, Rollett A D and Rohrer G S 2007 Recrystallization and Grain Growth III, Pts 1 and 2, ed S J L Kang, et al. pp 915-20

[11]　Saylor D M, Morawiec A and Rohrer G S 2003 Distribution of grain boundaries in magnesia as a function of five macroscopic parameters Acta Materialia 51 3663-74

[12]　Adams B L, Ta'asan S, Kinderlehrer D, Livshits I, Mason D E, Wu C T, Mullins W W, Rohrer G S, Rollett A D and Saylor D M 1999 Extracting grain boundary and surface energy from measurement of triple junction geometry Interface Sci 7 321-38